

# Alternating Minimization for Time-Shifted Synergy Extraction in Human Hand Coordination

Trevor Stepp, Parthan Olikkal, Ramana Vinjamuri, and Rajasekhar Anguluri

Department of Computer Science and Electrical Engineering,  
University of Maryland, Baltimore County, MD 21229 USA  
e-mails: {trevors3, polikka1, rvinjam1, rajangul}@umbc.edu

**Abstract:** Identifying motor synergies – coordinated hand joint patterns activated at task-dependent time shifts – from kinematic data is central to motor control and robotics. Existing two-stage methods first extract candidate waveforms (via SVD) and then select shifted templates using sparse optimization, requiring at least two datasets and complicating data collection.

We introduce an optimization-based framework that jointly learns a small set of synergies and their sparse activation coefficients. The formulation enforces group sparsity for synergy selection and element-wise sparsity for activation timing. We develop an alternating minimization method in which coefficient updates decouple across tasks and synergy updates reduce to regularized least-squares problems. Our approach requires only a single data set, and simulations show accurate velocity reconstruction with compact, interpretable synergies.

**Keywords:** Human hand coordination, Convolution-mixture model, Dimensionality reduction, Group LASSO, Alternating minimization.

## 1. INTRODUCTION

Our hand movements exhibit remarkable flexibility despite the high-dimensional nature of the musculoskeletal system. Coordinating dozens of joints and muscles in real time presents a challenging control problem. Yet, we perform grasping and manipulation tasks with ease, suggesting that the central nervous system exploits low-dimensional structure in hand motion. This idea is captured through the notion of *motor synergies*: coordinated patterns of hand joint movements that serve as building blocks for executing a wide range of tasks (see Bernstein (1967)).

A key question in motor control and robotics is therefore how to identify such synergies directly from measured kinematic data. Dimensionality reduction plays a key role here: representing hand motion using only a few synergies not only yields compact models but also provides interpretability relevant to neuroscience, prosthetics, human–robot interaction, and rehabilitation Vinjamuri et al. (2010, 2014).

Several computational methods have been proposed for synergy extraction, including PCA (d’Avella et al., 2006; Bizzi et al., 2008; Muceli et al., 2010), and tensor factorization techniques (Ebied et al., 2019; Kim et al., 2020; Chen et al., 2024). While these approaches have provided foundational insights, they typically assume linear mixing and do not naturally accommodate time-shifted, sparse, or temporally structured activation patterns. To address these limitations, time-varying and convolutional synergy models have been proposed (d’Avella and Bizzi, 2005; Chiovetto et al., 2022). Our prior work has also showed the importance of modeling temporal alignment, activation delays, and dynamic structure in synergy extraction (see

(Vinjamuri et al., 2010; Myrick et al., 2025)), showing that traditional linear factorization methods may miss critical components of the underlying sensorimotor organization.

This work introduces a structured, scalable optimization framework for simultaneous synergy extraction and velocity reconstruction based on a sparse, time-shifted representation of grasping kinematics. Unlike existing two-stage methods that require separate data sets for the same task (Vinjamuri et al., 2012), our framework operates on a single data set. Our main contributions are as follows:

- We develop a matrix-valued representation of hand velocities in which synergies appear through time-shifted activations encoded by Toeplitz matrices. This representation captures temporal structure that traditional matrix-factorization methods do not model.
- We formulate a sparse optimization problem to jointly identify a small set of synergies and task-dependent activation coefficients. Our formulation uses group- and element-wise sparsity, enabling automatic selection and pruning of inactive synergies.
- We develop an alternating minimization method (AMM) in which the coefficient updates decouple across tasks, and each synergy is updated through a separate Ridge regression. This structure enables the method to scale to large numbers of grasping tasks.

We validate the AMM on a natural-grasping dataset and an American Sign Language posture dataset, and compare its performance against the two-stage baseline. Our results show that AMM is an effective dimensionality-reduction tool for synergy selection, while reducing experimental data-collection requirements by roughly half.

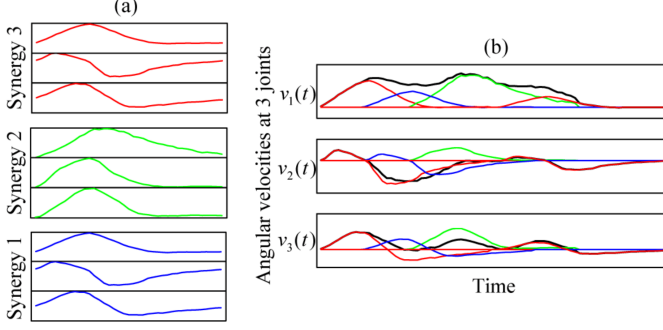


Fig. 1. Three synergies—each repeated three times in (a)—combine to produce hand velocities (shown in black) at all joints in (b). Reproduced from Vinjamuri et al. (2010).

## 2. PRELIMINARIES

As said in the introduction, we assume that the latent synergy waveforms combine linearly to produce the observed hand movement. Let  $v_i(t) \in \mathbb{R}$  denote the angular velocity of the  $i$ -th hand joint at time  $t \in \mathbb{R}$ . Vinjamuri et al. (2010) and the subsequent studies propose that

$$v_i^g(t) = \sum_{j=1}^m \sum_{k=1}^{K_j} c_{jk}^g s_i^j(t - t_{jk}), \quad i = 1, \dots, n \quad (1)$$

for a grasping task  $g \in \{1, \dots, G\}$ , where  $s_i^j(t)$  corresponds to the  $j$ -th kinematic synergy associated with  $i$ -th hand movement. Here  $K_j$  specifies how many times the  $j$ -th synergy is recruited, while  $c_{jk}^g$  and  $t_{jk}$  denote the nonnegative amplitude and time-shift parameters, respectively.

The outer sum in (1) indexes the  $m$  synergies. The inner sum indexes for multiple recruitments (repeats) of each synergy. Define the  $n$ -vector  $\mathbf{v}(t) = [v_1(t), \dots, v_n(t)]^\top$  of angular velocities, corresponding to the  $n$  hand joints at  $t$ . Then, for all  $n$ -joints, from (1) we have

$$\mathbf{v}^g(t) = \sum_{j=1}^m \sum_{k=1}^{K_j} c_{jk}^g \mathbf{s}^j(t - t_{jk}). \quad (2)$$

where each  $n$ -vector  $\mathbf{s}^j(t) = [s_1^j(t), s_2^j(t), \dots, s_n^j(t)]^\top \in \mathbb{R}^n$ . Fig. 1 visually displays the model in (2) for  $n = 3$  joints and  $m = 3$  synergies. In general,  $n \neq m$ .

The governing equation in (2) admits a natural convolutive-mixture model interpretation. We outline the central idea here; see Vinjamuri et al. (2008, 2010) for details. Let  $c_j(t)$  denote a train of impulses with amplitudes  $c_{jk}$  occurring at times  $t_{jk}$ , where  $k = 1, \dots, K_j$ . Then (2) becomes

$$\mathbf{v}^g(t) = \sum_{j=1}^m (c_j^g * \mathbf{s}^j)(t). \quad (3)$$

Here  $*$  is the standard convolution product for Linear Time Invariant signals.

**Problem Statement:** Given noisy measurements  $\mathbf{v}^g(t)$  for  $t = 1, \dots, T$  and  $g = 1, \dots, G$ , identify the smallest number of synergies  $m$  and the fewest recruitments  $K_j$  per synergy that jointly explain the observed hand angular-velocity data across all  $G$  tasks.

## 3. A MATRIX-VALUED MODEL

Since our goal is to learn synergy waveforms common to the  $G$  grasping tasks over a window of size  $T$ , we stack the time-indexed  $\mathbf{v}^g(t)$  in (2) to obtain a matrix-valued model of the activation coefficients and synergies. First, we express the time-shifted synergies using shift matrices by assuming that the synergy duration satisfies  $T_s \leq T$ . This condition ensures that each synergy can be embedded into the observation window without truncation.

Form the  $T_s$ -dimensional vector  $\mathbf{s}_i^j = [s_i^j(1), \dots, s_i^j(T_s)]^\top$  by stacking over time the  $i$ -th element of the  $j$ -th synergy (see (1)). Define the template vector for the  $j$ -th synergy:

$$\mathbf{s}_{[1:T_s]}^j \triangleq \begin{bmatrix} \mathbf{s}_1^j \\ \vdots \\ \mathbf{s}_n^j \end{bmatrix} \in \mathbb{R}^{nT_s}, \quad j \in \{1, \dots, m\}. \quad (4)$$

Let  $t_{jk} \geq 0$  be the  $k$ -th shift or recruitment associated with the  $j$ -th synergy. Define the  $nT$ -dimensional time-shifted vector  $\mathbf{s}_{[1-t_{jk}:T-t_{jk}]}^j$  similar to (4). Then there exists an  $(nT) \times (nT_s)$  matrix  $\mathbf{D}_{jk}$  of zeros and ones such that

$$\mathbf{s}_{[1-t_{jk}:T-t_{jk}]}^j = \mathbf{D}_{jk} \mathbf{s}_{[1:T_s]}^j. \quad (5)$$

Henceforth, we drop the subscript notation from  $\mathbf{s}_{[1:T_s]}^j$ . In essence,  $\mathbf{D}_{jk}$  implements the time-shift by selecting and placing entries of  $\mathbf{s}^j$  into the correct time slots, with zeros filling the remaining positions (see Example 1).

So far our attention was on stacking time-indexed vectors. We focus on the spatial terms (that is, the number of synergies  $m$  and their recruits). For the  $j$ -th synergy, define the matrix of time-shifted vectors given by (5):

$$\mathbf{D}(\mathbf{s}^j) \triangleq [\mathbf{D}_{j1} \mathbf{s}^j | \mathbf{D}_{j2} \mathbf{s}^j | \dots | \mathbf{D}_{jK_j} \mathbf{s}^j] \in \mathbb{R}^{nT \times K_j}.$$

Let  $\mathbf{c}_j^g = [c_{j1}^g, \dots, c_{jK_j}^g]^\top$  be the vector of scalar coefficients multiplying the vectors  $\mathbf{s}_i^j(t - t_{jk})$  in (2). Then the matrices  $\mathbf{D}(\mathbf{s}^j)$  provide an efficient representation of the convolution model in (3). In particular,

$$\sum_{k=1}^{K_j} c_{jk}^g \mathbf{s}^j(t - t_{jk}) = \mathbf{D}(\mathbf{s}^j) \mathbf{c}_j^g. \quad (6)$$

As illustrated in Example 1, this matrix–vector product is a Toeplitz matrix acting on a coefficient vector, i.e., a convolution sum unfolded over the  $T$  time instants.

*Example 1.* We now present a toy model to visualize the matrices and vectors defined above. Our setup contains:  $G = 4$  tasks, synergy duration of  $T_s = 3$ , and a movement duration of  $T = 6$ . Each synergy admits  $K_j = T - T_s + 1 = 4$  possible time shifts. For simplicity, the  $k$ -th time-shift value  $t_{jk} = k$ .

Consider the case  $n = m = 1$ . Let the shifting index  $k = 4$ . The unshifted synergy segment ( $nT_s = 3$ ) is

$$\mathbf{s}_{[1:T_s]}^j = \begin{bmatrix} \mathbf{s}^j(1) \\ \mathbf{s}^j(2) \\ \mathbf{s}^j(3) \end{bmatrix} \in \mathbb{R}^3.$$

Note that  $j = 1$ ; but we retain the notation  $j$ . The time-shifted synergy vector of length  $nT = 6$  is

$$\mathbf{s}_{[1-t_{jk}:T-t_{jk}]}^j = \begin{bmatrix} \mathbf{0}_3 \\ \mathbf{s}^j(1) \\ \mathbf{s}^j(2) \\ \mathbf{s}^j(3) \end{bmatrix} \in \mathbb{R}^6,$$

where entries with indices outside  $\{1, \dots, T_s\}$  are set to zero. This shift is given by the matrix:

$$\mathbf{D}_{j4} = \begin{bmatrix} \mathbf{0}_{3 \times 3} \\ \mathbf{I}_{3 \times 3} \end{bmatrix}, \quad \mathbf{s}_{[1-t_{jk}:T-t_{jk}]}^j = \mathbf{D}_{j4} \mathbf{s}_{[1:T_s]}^j.$$

Stacking the time-shifted versions of the synergy  $\mathbf{s}^j$  for all  $K_j = 4$  shifts yields a Toeplitz-like matrix:

$$\begin{aligned} \mathbf{D}(\mathbf{s}^j) &= [\mathbf{D}_{j1}\mathbf{s}^j \mid \mathbf{D}_{j2}\mathbf{s}^1 \mid \mathbf{D}_{j3}\mathbf{s}^j \mid \mathbf{D}_{j4}\mathbf{s}^j] \\ &= \begin{bmatrix} \mathbf{s}^1(1) & 0 & 0 & 0 \\ \mathbf{s}^1(2) & \mathbf{s}^1(1) & 0 & 0 \\ \mathbf{s}^1(3) & \mathbf{s}^1(2) & \mathbf{s}^1(1) & 0 \\ 0 & \mathbf{s}^1(3) & \mathbf{s}^1(2) & \mathbf{s}^1(1) \\ 0 & 0 & \mathbf{s}^1(3) & \mathbf{s}^1(2) \\ 0 & 0 & 0 & \mathbf{s}^1(3) \end{bmatrix}. \end{aligned}$$

The velocity vector in (7) becomes

$$\begin{bmatrix} \mathbf{v}^g(1) \\ \mathbf{v}^g(2) \\ \vdots \\ \mathbf{v}^g(6) \end{bmatrix} = \mathbf{D}(\mathbf{s}^j) \mathbf{c}_j^g = \begin{bmatrix} \mathbf{s}^1(1)c_{j1}^g \\ \mathbf{s}^1(2)c_{j1}^g + \mathbf{s}^1(1)c_{j2}^g \\ \vdots \\ \mathbf{s}^1(3)c_{jK}^g \end{bmatrix},$$

which is nothing but the convolution sum expressed for all  $T = 6$  instants.

For  $n = 2$  joint synergy vector of dimension  $nT_s = 6$ , the shift matrix is obtained by applying the same temporal synergy vector independently to each joint.

For a grasping task  $g \in \{1, \dots, G\}$ , define the time-stacked vector of velocities  $\mathbf{v}_{1:T}^g = [(\mathbf{v}^g(1))^\top \dots (\mathbf{v}^g(T))^\top]^\top$ . From (2) and (6), it then follows that

$$\mathbf{v}_{1:T}^g = \sum_{j=1}^m \mathbf{D}(\mathbf{s}^j) \mathbf{c}_j^g. \quad (7)$$

Grasping velocity measurements are corrupted by additive sensor noise, so the model in (7) can be augmented as

$$\mathbf{v}_{1:T}^g = \sum_{j=1}^m \mathbf{D}(\mathbf{s}^j) \mathbf{c}_j^g + \boldsymbol{\epsilon}^g. \quad (8)$$

The set of matrices  $\{\mathbf{D}(\mathbf{s}^j)\}_{j=1}^m$  is constant for all grasping tasks. We drop the subscript notation from  $\mathbf{v}_{1:T}^g$ . Finally, define  $\{\mathbf{s}^j\} \triangleq \{\mathbf{s}^1, \dots, \mathbf{s}^m\}$ ; and  $\{\mathbf{c}_j^g\} \triangleq \{\mathbf{c}_1^g, \dots, \mathbf{c}_m^g\}$ , for all grasping tasks  $g \in \{1, \dots, G\}$ .

#### 4. OPTIMIZATION PROBLEM

For the model in (8), and using only the observed grasping velocities  $\mathbf{v}^1, \dots, \mathbf{v}^G$ , we seek to estimate:

- (1) the synergy vectors  $\mathbf{s}^1, \dots, \mathbf{s}^m$ , under the assumption that only a small subset of these synergies is required to explain all grasping tasks;
- (2) the coefficients  $\{\mathbf{c}_j^g\}$  for each task  $g$ , assuming that each task activates only a few time-shifted synergies.

These estimation goals can be formulated as an optimization problem equipped with regularizers (on the coefficient vectors  $\mathbf{c}_1^g$ ). In particular, we solve

$$\begin{aligned} \arg \min_{\{\mathbf{s}^j\}, \{\mathbf{c}_1^1\}, \dots, \{\mathbf{c}_1^G\}} \quad & \sum_{g=1}^G \left\{ \frac{1}{2} \|\mathbf{v}^g - \sum_{j=1}^m \mathbf{D}(\mathbf{s}^j) \mathbf{c}_j^g\|_2^2 \right. \\ & \left. + \lambda \mathcal{R}(\{\mathbf{s}^j\}) + \sum_{j=1}^m \|\mathbf{c}_j^g\|_{\ell_2/\ell_1} \right\}, \quad (9) \end{aligned}$$

where  $\|\mathbf{x}\|_{\ell_2/\ell_1} \triangleq \lambda_1 \|\mathbf{x}\|_2 + \lambda_2 \|\mathbf{x}\|_1$  is the sparse group LASSO norm (norms are not squared); and  $\lambda, \lambda_1, \lambda_2 \geq 0$ .

The first term in (9) is the squared  $\ell_2$  loss. The second ensures that the learned synergies represent smooth patterns. We set  $\mathcal{R}(\{\mathbf{s}^j\}) = \sum_j \|\mathbf{s}^j\|_2^2$ . The last combines  $\ell_2$  and  $\ell_1$  norms to promote sparsity at two levels: only a few synergies are used (group sparsity), and each selected synergy is activated only a few time shifts (element-wise sparsity).

If the problem in (9) is solved successfully, many coefficient vectors  $\{\mathbf{c}_j^g\}$  become zero, yielding automatic dimensionality reduction. The remaining nonzero vectors are sparse, so the velocity in (2) is captured by only a few synergies and a small number of time-shifted activations. We present an alternating-minimization method for solving (9).

#### 4.1 Alternating Minimization Method (AMM)

The problem in (9) is non-convex and non-differentiable. The non-convexity arises from the bilinear terms  $\mathbf{D}(\mathbf{s}^j) \mathbf{c}_j^g$ , where both factors are unknown. The non-differentiability stems from the  $\ell_2$  and  $\ell_1$  regularizers, although this issue is well-handled by modern optimization techniques. To address the non-convexity, we employ AMM, wherein we iteratively update  $\{\mathbf{c}_j^g\}$  and  $\{\mathbf{s}^j\}$  while holding the other fixed.

AMM begins by randomly initializing  $m = m_{\text{int}}$  synergies. If the AMM is converged and successful, we end up with fewer ( $m_{\text{final}} \ll m_{\text{int}}$ ) synergies.

*C-step (coefficient update):* Given the estimates of  $\{\hat{\mathbf{s}}^j\}$ , we update the coefficients by solving (9) over  $\{\mathbf{c}_j^g\}$ . Since  $\mathcal{R}(\cdot)$  acts only on  $\{\hat{\mathbf{s}}^j\}$ , it is constant in this step and is dropped. The resulting optimization decouples across grasping tasks and can therefore be solved independently for each  $g$ .

$$\{\hat{\mathbf{c}}_j^g\} \leftarrow \arg \min_{\{\mathbf{c}_j\}} \frac{1}{2} \|\mathbf{v}^g - \sum_{j=1}^m \mathbf{D}(\hat{\mathbf{s}}^j) \mathbf{c}_j\|_2^2 + \sum_{j=1}^m \|\mathbf{c}_j\|_{\ell_2/\ell_1}. \quad (10)$$

This is a convex optimization problem and can be solved efficiently (Simon et al., 2013). The penalty performs dimensionality reduction by driving entire sets of coefficients associated with a synergy to zero; see Remark 1.

*S-step (synergies update):* Given  $\{\hat{\mathbf{c}}_j^g\}$ , for  $g \in \{1, \dots, G\}$ , we solve the problem below after dropping the constant term (for this step):

$$\{\hat{\mathbf{s}}^j\} \leftarrow \arg \min_{\{\mathbf{s}^j\}} \sum_{g=1}^G \frac{1}{2} \|\mathbf{v}^g - \sum_{j=1}^m \mathbf{D}(\mathbf{s}^j) \hat{\mathbf{c}}_j^g\|_2^2 + \frac{\alpha}{2} \sum_{j=1}^m \|\mathbf{s}^j\|_2^2, \quad (11)$$

where we set  $\lambda = \alpha/2G \geq 0$ .

At the outset, solving (11) appears challenging. First,  $\mathbf{s}^j$  influence every task, so the  $l_2$  loss couples all  $G$  summands, which could be large. Second, each  $\mathbf{D}(\mathbf{s}^j)$  is an  $nT \times K_j$  Toeplitz matrix whose size grows with the number of shifts  $K_j$ , making a naive implementation expensive. After some algebra, we show that the problem in (11) can be solved efficiently, one synergy  $\mathbf{s}^j$  at a time, by reducing it to a simple  $\ell_2$ -regularized least-squares (i.e., a Ridge regression).

For any  $j \in \{1, \dots, m\}$ , define the residual for the task  $g$  excluding the  $j$ -th synergy:

$$\mathbf{r}_{-j}^g = \mathbf{v}^g - \sum_{\ell \neq j} \mathbf{D}(\mathbf{s}^\ell) \hat{\mathbf{c}}_\ell^g, \quad g = 1, \dots, G.$$

By direct inspection, for any fixed synergy vector  $\mathbf{s}^j$ ,

$$\mathbf{D}(\mathbf{s}^j) \hat{\mathbf{c}}_j^g = \left( \sum_{k=1}^{K_j} \hat{\mathbf{c}}_{jk}^g \mathbf{D}_{jk} \right) \mathbf{s}^j, \quad g = 1, \dots, G.$$

Let  $\mathbf{B}_j(\hat{\mathbf{c}}_j^g)$  denote the matrix in parentheses to the right, which is known because  $\hat{\mathbf{c}}_j^g$  is known.

Stack the quantities across the  $G$  tasks:

$$\mathbf{r}_{-j} = \begin{bmatrix} \mathbf{r}_{-j}^1 \\ \vdots \\ \mathbf{r}_{-j}^G \end{bmatrix} \in \mathbb{R}^{nTG}, \quad \mathbf{B}_j = \begin{bmatrix} \mathbf{B}_j(\hat{\mathbf{c}}_j^1) \\ \vdots \\ \mathbf{B}_j(\hat{\mathbf{c}}_j^G) \end{bmatrix} \in \mathbb{R}^{(nTG) \times (nT_s)}.$$

The update for the  $j$ -th synergy reduces to Ridge regression:

$$\hat{\mathbf{s}}^j \leftarrow \arg \min_{\hat{\mathbf{s}}} \frac{1}{2} \|\mathbf{r}_{-j} - \mathbf{B}_j \hat{\mathbf{s}}\|_2^2 + \frac{\alpha}{2} \|\hat{\mathbf{s}}\|_2^2,$$

where  $\hat{\mathbf{s}}$  has the same dimension as  $\mathbf{s}^j$ .

After each update, we normalize  $\mathbf{s}^j$  and rescale  $\mathbf{c}_j^g$  accordingly to remove scaling ambiguity.

*Remark 1.* For synergy extraction, we may use only the group LASSO regularizer (i.e., set  $\lambda_2 = 0$  in (9)) instead of the full sparse-group penalty. Nevertheless, we found that using the sparse group lasso during training improves generalization during testing. Specifically, it activates only a few shifts for the active synergies.  $\square$

## 5. RESULTS AND DISCUSSION

We evaluate the performance of the AMM on hand grasping data and compare it against the two-stage approach of Vinjamuri et al. (2010). Our simulations use the natural-grasp dataset, in which subjects<sup>1</sup> grasp objects of various shapes and sizes while wearing a right-handed CyberGlove that records joint-angle measurements. We focus on ten joints: the MCP and IP joints of the thumb and the MCP and PIP joints of the four fingers, which capture the dominant kinematic patterns in the grasping tasks.

AMM uses only the natural-grasp dataset for both synergy extraction and coefficient estimation. In contrast, the two-stage baseline requires an additional rapid-grasp dataset to extract synergies (via SVD) before estimating coefficients from natural grasps, doubling the data-collection effort. Datasets were generated through real-time experiments conducted by one of the authors in prior work (Vinjamuri et al., 2010, 2012).

<sup>1</sup> We consider a total of seven subjects in this work.

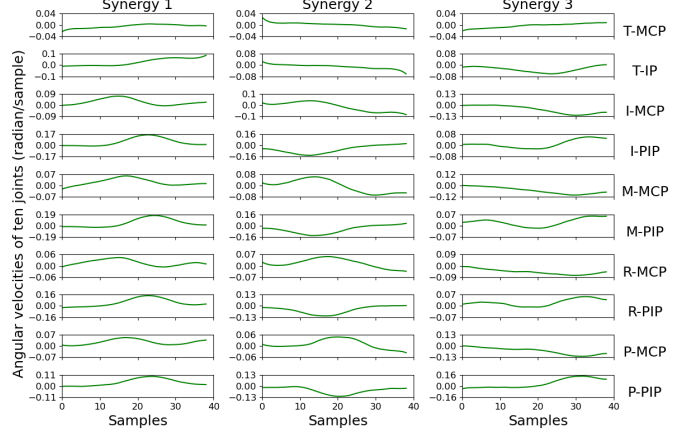


Fig. 2. Joint angular-velocity profiles of three synergies among the seven extracted using AMM. The smoothness of the profiles are due to the smoothing penalty term  $\mathcal{R}(\cdot)$  in (9). Abbreviations: T, thumb; I, index finger; M, middle finger; R, ring finger; P, pinky finger; MCP, metacarpophalangeal joint; IP, interphalangeal joint; PIP, proximal IP joint.

### 5.1 Synergy Extraction and Coefficient Estimation

Each grasp consists of  $T = 82$  time samples across  $n = 10$  joints, yielding  $G = 100$  grasping tasks. We set  $m_{\text{int}} = 10$  candidate synergies, each of duration  $T_s = 39$  samples. These synergies are then shifted and embedded into the observation window as described in Section 3. This gives each synergy  $K_j = T - T_s + 1 = 44$  possible time shifts. Thus, for ten joints, the coefficient vector associated with the  $j$ -th synergy in task  $g$  is 440-dimensional. The tuning parameters ( $\lambda, \lambda_1, \lambda_2$  in (9)) for the sparse group LASSO and the ridge regression were selected using a small grid search over a discrete set of reasonable values.

AMM discarded three synergies that remained inactive across all 100 grasping tasks, yielding  $m_{\text{final}} = 7$  synergies. The joint angular-velocity profiles of three of these synergies for Subject 2 are in Fig. 2. Each row corresponds to one of the ten joints. As expected, the synergy waveforms are smooth functions of time with peaks and valleys marking periods of hand acceleration and deceleration.

To visualize each synergy's temporal postures (that is, the corresponding hand movements), we recover joint angles by discretely integrating the joint angular velocities. The seven resulting postural synergies are displayed in Fig. 3. Each synergy is illustrated using five snapshots at 0%, 25%, 50%, 75%, and 100% of the task duration, revealing how the hand configuration evolves over the course of the movement. The end posture is particularly informative, as it reflects the specific hand configuration that each synergy contributes toward achieving a given grasp.

We compare the (end) postural synergies obtained using AMM with those reported by the two-stage baseline in Vinjamuri et al. (2010). Although the baseline estimates synergies from the rapid-grasp dataset, the comparison is valid because both rapid and natural grasps involve the same set of grasping tasks. In Fig. 3 and (Vinjamuri et al., 2010, Fig. 6a), we observe three dominant terminal postures: (1) a whole-hand (power) grasp, characterized by simultaneous flexion of all digits; (2) a two-finger pinch,

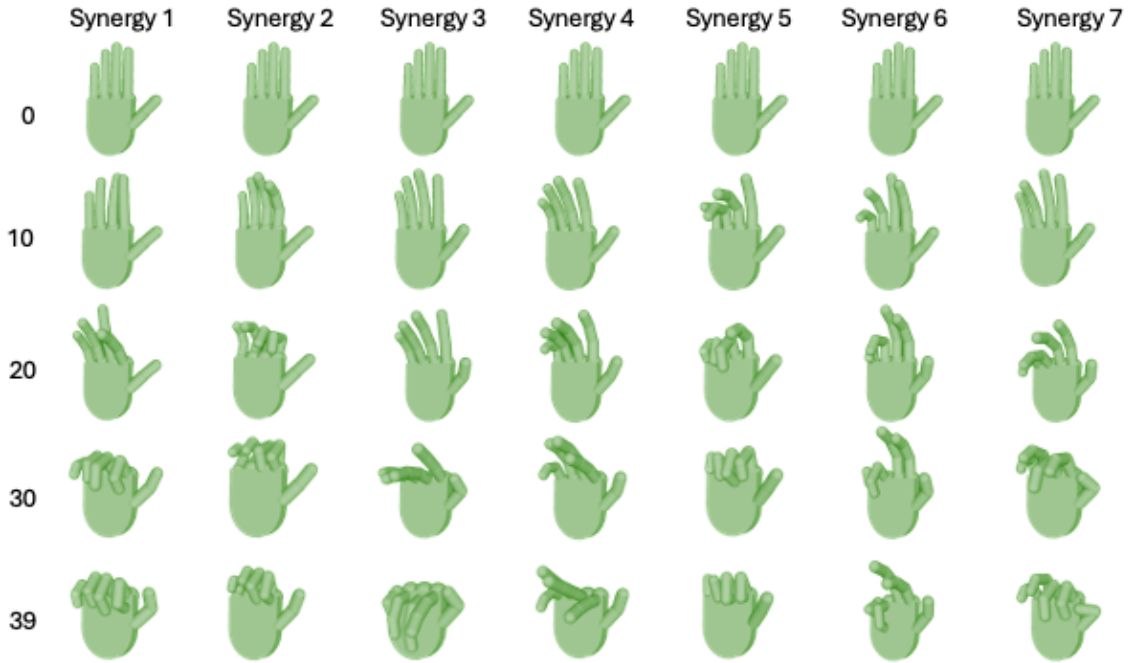


Fig. 3. Joint angle profiles of the seven synergies at time steps 0, 10, 20, 30, and 39. Columns represent synergies and rows represent the time steps. Each hand posture is produced by coordination of ten finger joints. For instance, in Synergy 7, the MCP and IP joints of the thumb and the MCP and PIP joints of the other four fingers combine to form the common two-finger pinch posture.

primarily involving coordinated flexion of the thumb and index finger; and (3) a full-hand extension posture in which all digits return to an extended configuration.

The emergence of these same temporal postures across studies – despite differences in synergy extraction methods – highlights a fundamental underlying structure in human hand control. Importantly, the fact that these archetypal postures arise from both standard SVD (Vinjamuri et al., 2010) and our joint estimation problem in (9) (current work) demonstrates that each method converges on a set of anatomically and functionally meaningful synergies.

## 5.2 Reconstruction of Hand Movements

By combining synergy velocities (shown in Fig. 2) with their estimated time-shifted coefficients (not shown) as in model (1), we obtain reconstructed joint velocities. The difference between these reconstructions and the measured velocities yields the training error. While important, we shall not focus on training error as our interest is in how well the learned synergies generalize to unseen grasps. We therefore turn to testing-phase reconstruction.

In the testing phase, we use the American Sign Language (ASL) dataset described in Vinjamuri et al. (2010). This dataset consists of 36 ASL gestures (the digits 0-9 and the letters A-Z), collected using the same Cyber-Glove and the same ten selected joints as in training. This choice of the data serves two purposes: (i) it broadens the scope of our evaluation, and (ii) it highlights the core idea behind synergies: they act as basic building blocks of movement. Once learned from one set of tasks (e.g., natural grasping),

the same synergies can be used to reconstruct entirely different types of hand motions, such as ASL gestures.

Accordingly, for both our method and the two-stage baseline, we use the synergies learned during training. The activation coefficients from training are not reused; in the testing phase, these coefficients are the unknowns and are determined by solving the  $\ell_1$ -regularized least-squares:

$$\hat{\mathbf{c}}^g \leftarrow \arg \min_{\mathbf{c}^g} \frac{1}{2} \left\| \mathbf{v}_{\text{test}}^g - \mathbf{B}^\top \mathbf{c}^g \right\|_2^2 + \lambda_{\text{test}} \|\mathbf{c}^g\|_1, \quad (12)$$

for each testing gesture<sup>2</sup>  $g = 1, \dots, 36$ , with  $\lambda_{\text{test}} \geq 0$ . Here  $\mathbf{v}_{\text{test}}^g \in \mathbb{R}^{nT}$  is the measured angular-velocity trajectory for the testing data, obtained by concatenating the  $n = 10$  joint velocities over the testing duration ( $T = 86$  samples). The matrix  $\mathbf{B}$  is the bank of time-shifted synergies arranged in the canonical order described in Vinjamuri et al. (2012). Under an appropriate permutation, one can verify that  $\mathbf{B}\mathbf{c}^g$  recovers the linear model in (7) (see Remark 2).

Once  $\hat{\mathbf{c}}^g$  is obtained, the model in (1) is used to reconstruct the joint velocities, which are then compared with the measured testing velocities to compute the reconstruction error. A smaller error indicates that the mixture model captures the underlying hand movements and that the estimation procedure (AMM or the two-stage baseline) successfully identifies its parameters.

The (normalized) reconstruction error for each ASL gesture  $g$  is defined as in Vinjamuri et al. (2010):

<sup>2</sup> In the ASL dataset, each movement is termed a gesture rather than a grasping task, but we retain the notation  $g$  for indexing.

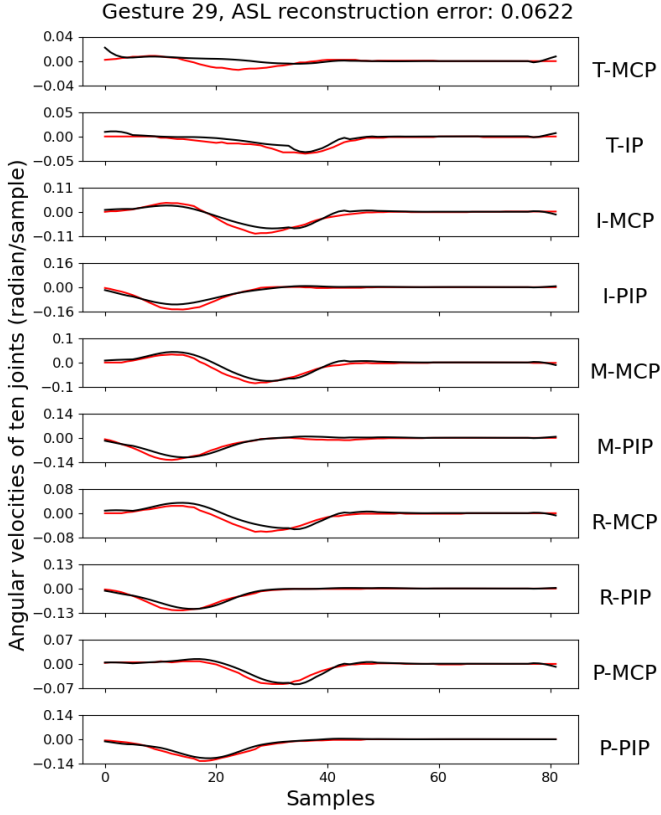


Fig. 4. Joint angular velocity of an ASL gesture (red line) and our model’s reconstruction (black line) using seven synergies. See Fig. 2 for abbreviations of finger joints.

$$\frac{\sum_{i=1}^n \sum_{t=1}^T [v_i^g(t) - \hat{v}_i^g(t)]^2}{\sum_{i=1}^n \sum_{t=1}^T v_i^g(t)^2},$$

where  $v_i^g(t)$  denotes the measured angular velocity of joint  $i$  at time  $t$ , and  $\hat{v}_i^g(t)$  is its reconstructed counterpart. For the 36 ASL gestures ( $g = 1, \dots, 36$ ), the per-subject average reconstruction errors are reported in Table 1. Across all seven subjects, the global average reconstruction error is 0.2783 with a standard deviation (std) of 0.02153. For a fixed set of seven synergies, this average error is comparable to that reported for the baseline two-stage method (Vinjamuri et al., 2010, Fig. 8b).

Table 1. Average reconstruction errors of 36 ASL gestures for each subject.

Subject 1	Subject 2	Subject 3	Subject 4
0.2587	0.2799	0.2803	0.2486
Subject 5	Subject 6	Subject 7	Avg error (std)
0.2976	0.3113	0.2715	<b>0.2783 (0.02153)</b>

An example of a successful reconstruction for a particular ASL movement is depicted in Fig. 4, with the corresponding temporal postures at selected time points in Fig. 5. Both figures use synergies extracted from Subject 2’s natural-grasping data to reconstruct the ASL gesture sequence from the same subject.

*Remark 2. (Implementation Details)* Before solving the velocity reconstruction problem in (12), we mitigate multicollinearity in the synergy bank matrix  $\mathbf{B}^\top$  by removing shifts whose pairwise correlation exceeds a threshold

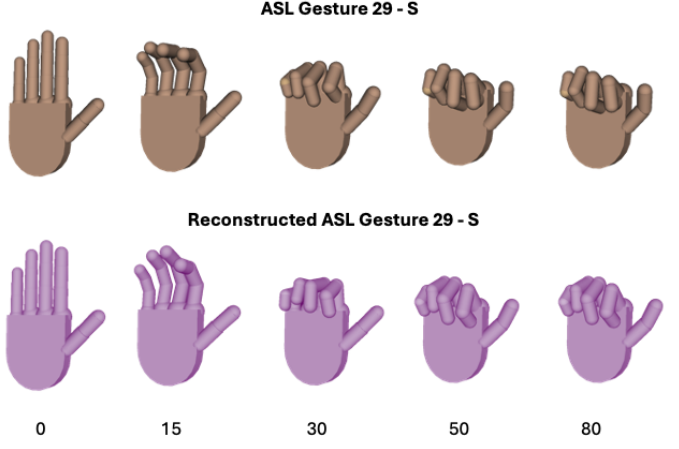


Fig. 5. Joint angle profiles of ASL gesture 29 (the letter *S*) and our model’s reconstruction at time steps 0, 15, 30, 50, and 80.

$\tau = 0.8$ . This reduces multicollinearity in  $\mathbf{B}^\top$ , which otherwise can lead to inconsistent coefficient estimates during testing. To ensure that the reconstructed velocities remain smooth functions of time, we apply a Savitzky–Golay filter to the columns of the resulting matrix  $\mathbf{B}^\top$ .  $\square$

## 6. CONCLUSION

This work introduced a group-sparsity–based optimization framework for learning time-shifted hand synergies and reconstructing joint velocities from kinematic data. Central to this framework is a matrix-valued nonlinear equation that links the observed data to the synergy waveforms and their time-shifted activation coefficients. We developed an iterative method that updates activation coefficients across tasks and refines synergy waveforms through independent Ridge regressions. Experiments on natural-grasping and ASL posture datasets demonstrate that our method extracts compact and interpretable synergies while achieving accurate velocity reconstruction.

The numerical results are encouraging and point to several directions for future work: developing convergence guarantees for AMM, exploring structure-promoting regularization schemes, and extending the framework to multimodal or higher-dimensional datasets. Improving computational scalability may also enable applications in sports performance, rehabilitation, and motor-skill training.

## REFERENCES

Bernstein, N.A. (1967). *The Co-Ordination and Regulation of Movements*. Pergamon Press, Oxford.

Bizzi, E., Cheung, V.C., d’Avella, A., Saltiel, P., and Tresch, M. (2008). Combining modules for movement. *Brain research reviews*, 57(1), 125–133.

Chen, X., Feng, Y., Chang, Q., Yu, J., Chen, J., and Xie, P. (2024). Muscle synergy during wrist movements based on non-negative Tucker decomposition. *Sensors*, 24(10), 3225.

Chiavetto, E., Salatiello, A., d’Avella, A., and Giese, M.A. (2022). Toward a unifying framework for the modeling and identification of motor primitives. *Frontiers in Computational Neuroscience*, 16, 926345.

d'Avella, A. and Bizzi, E. (2005). Shared and specific muscle synergies in natural motor behaviors. *Proceedings of the national academy of sciences*, 102(8), 3076–3081.

d'Avella, A., Portone, A., Fernandez, L., and Lacquaniti, F. (2006). Control of fast-reaching movements by muscle synergy combinations. *Journal of Neuroscience*, 26(30), 7791–7810.

Ebied, A., Kinney-Lang, E., Spyrou, L., and Escudero, J. (2019). Muscle activity analysis using higher-order tensor decomposition: Application to muscle synergy extraction. *IEEE Access*, 7, 27257–27271.

Kim, Y., Stapornchaisit, S., Miyakoshi, M., Yoshimura, N., and Koike, Y. (2020). The effect of ica and non-negative matrix factorization analysis for emg signals recorded from multi-channel emg sensors. *Frontiers in Neuroscience*, 14, 600804.

Muceli, S., Boye, A.T., d'Avella, A., and Farina, D. (2010). Identifying representative synergy matrices for describing muscular activation patterns during multidirectional reaching in the horizontal plane. *Journal of neurophysiology*, 103(3), 1532–1542.

Myrick, C., Vinjamuri, R., and Anguluri, R. (2025). Robust pca-based dimensionality reduction in human hand coordination. In *IEEE-EMBS International Conference on Body Sensor Networks 2025*.

Simon, N., Friedman, J., Hastie, T., and Tibshirani, R. (2013). A sparse-group lasso. *Journal of computational and graphical statistics*, 22(2), 231–245.

Vinjamuri, R., Crammond, D.J., Kondziolka, D., Lee, H.N., and Mao, Z.H. (2008). Extraction of sources of tremor in hand movements of patients with movement disorders. *IEEE Transactions on Information Technology in Biomedicine*, 13(1), 49–56.

Vinjamuri, R., Patel, V., Powell, M., Mao, Z.H., and Crone, N. (2014). Candidates for synergies: linear discriminants versus principal components. *Computational intelligence and neuroscience*, 2014(1), 373957.

Vinjamuri, R., Sun, M., Chang, C.C., Lee, H.N., Sclabassi, R.J., and Mao, Z.H. (2010). Dimensionality reduction in control and coordination of the human hand. *IEEE transactions on biomedical engineering*, 57(2), 284–295.

Vinjamuri, R., WeiWang, Sun, M., and Mao, Z.H. (2012). Application of linear and nonlinear dimensionality reduction methods. In P. Sanguansat (ed.), *Principal Component Analysis*, chapter 6. IntechOpen, London.